RPE | Radiation Physics & Engineering
An International Peer-Reviewed Journal
Published by K.N. Toosi University of Technology
http://rpe.kntu.ac.ir
Research Article

Radiation Physics and Engineering 2022; 3(3):39–45
https://doi.org/10.22034/RPE.2022.337683.1078

Investigation of the use of momentum and Galerkin weighting functions in high-order Nodal expansion method to solve the neutron diffusion equation

Ali Kolali, Davod Naghavi Dizaji*, Naser Vosoughi

Department of Energy Engineering, Sharif University of Technology, P.O. Box 14565-1114, Tehran, Iran

HIGHLIGHTS

- Development of high-speed and accurate steady-state neutronic simulator using the high-order nodal expansion method.
- Use of polynomials with Momentum and Galerkin weighting functions in discretization of neutron diffusion equation.
- These weighting functions for rectangular and hexagonal geometries can be used to discretize equations.
- It was concluded that accuracy increases within the acceptable time of computing.

ABSTRACT

In this study, after discretization of the neutron diffusion equation and adjoint with high-order nodal expansion method in two dimensions and two energy groups, calculations with Momentum and Galerkin weighting functions for rectangular geometry (BIBLIS-2D) and hexagonal geometry (IAEA-2D) reactors are performed. The mean of relative power error for Momentum and Galerkin weighting functions was calculated in BIBLIS-2D reactor 0.42% and 0.62%, respectively, and for IAEA-2D reactor 4.96% and 3.52%, respectively. Regarding the results, it was concluded that in order to increase accuracy with the acceptable time of computing (4 Seconds for rectangular geometry and 28 seconds for hexagonal geometry with Intel® Core™ i7-4510U Processor), the Momentum weighting function for rectangular geometry and the Galerkin weighting function for hexagonal geometry can be used to discretize equations without reducing the node size. Therefore, to increase the accuracy while maintaining the speed of calculations, without reducing the size of nodes, the appropriate weighting function can be used in discretization, which can be very useful in performing calculations of different transients.

KEYWORDS

Simulator
Adjoint calculation
Diffusion equation
Rectangular geometry
Hexagonal geometry
HACNEM

HISTORY

Received: 15 April 2022
Revised: 8 June 2022
Accepted: 11 June 2022
Published: Summer 2022

Nomenclature

Symbol	Meaning
$\phi_g(r)$	Neutron flux in the energy group g
$\overrightarrow{J}_g$	Neutron current in the energy group g
$\Sigma_{r,g}$	Macroscopic removal cross section in the energy group g
$\Sigma_{s,g'g}$	Macroscopic scattering cross section from energy group g' to g
$\Sigma_{f,g}$	Macroscopic fission cross section in the energy group g
k_{eff}	Neutron multiplication factor
ν_g	Fission neutron yield in the energy group g
h	Lattice pitch
Γ^m_{ws}	Left ($s=l$)/right ($s=r$) w-surface of the node m, $w=x,u,v$
Φ^m_g	Average flux for energy group g in the node m
Ψ^m_{gws}	Average flux for energy group g at Γ^m_{ws}
j^{+m}_{gws}	Average outgoing partial currents for group g at Γ^m_{ws}
j^{-m}_{gws}	Average incoming partial currents for group g at Γ^m_{ws}
e^m_{ws}	The unit vector in the direction of the outward normal to Γ^m_{ws}
A^m_{ws}	Area of Γ^m_{ws}
Π^{mws}	Node adjacent to the surface Γ^m_{ws}
$h_i(\xi)$	The polynomial of degree i of ξ_w and $\xi \cong \frac{w}{h}$
$\mathrm{d}\Pi^m$ and $\mathrm{d}\Gamma^m_{ws}$	The spatial dimensions in the nodal volume and surface
d_{gw}	High-order coefficients for hexagonal geometry, $w=x,u,v$
$\phi^\dagger$	Adjoint flux distribution
$k^\dagger_{\text{eff}}$	Adjoint multiplication factor

*Corresponding author: naghavi@energy.sharif.edu

1 Introduction

One of the basic needs in designing, simulating, and studying nuclear reactors is neutronic analysis. There are various numerical methods such as finite difference, finite volume, finite element, and nodal for spatial discretization of the neutron diffusion equation. Each of these methods can be used according to the desired geometry, the type, and size of the meshes, the required accuracy, and the desired computational time (Bell and Glasstone, 1970; Putney, 1986; Kolali et al., 2021; Hosseini et al., 2018; Lawrence, 1983; Finnemann, 1975).

Today in nuclear reactor calculations, researchers are looking for methods that, in addition to the acceptable accuracy, have optimal calculation cost. In order to have tools with optimal computational cost, a method that uses large nodes about the size of the fuel assemblies must be used, which shows the importance of using the nodal expansion method (NEM) in this type of calculation (Kolali et al., 2021; Hosseini et al., 2018; Lawrence, 1983; Finnemann, 1975; Hall, 2013). One of the ways to increase the accuracy of calculations without reducing the node size in the nodal expansion method is the use of suitable weighting functions.

There are different types of nodal methods with different basic functions, such as the nodal flux expansion method, analytical nodal method, method of expansion of analytical functions, nodal method of the Green function, etc. Among these methods, the nodal flux expansion method is the simplest and most stable method, but is less accurate (Hall, 2013; Sims, 1977; Hosseini and Vosoughi, 2012). Therefore, the main challenge of the nodal expansion method is its relatively low accuracy. In this paper, using the High-order nodal expansion method and nodes with the size of fuel assemblies, the accuracy of the calculations increases significantly.

In this study, by using different momentum and Galerkin weighting functions in the average current nodal expansion method (ACNEM) without reducing the size of the nodes, the accuracy of forward and adjoint calculations increases both locally (relative power distribution) and in general (effective multiplication factor). Also, the results of these two weighting functions are compared.

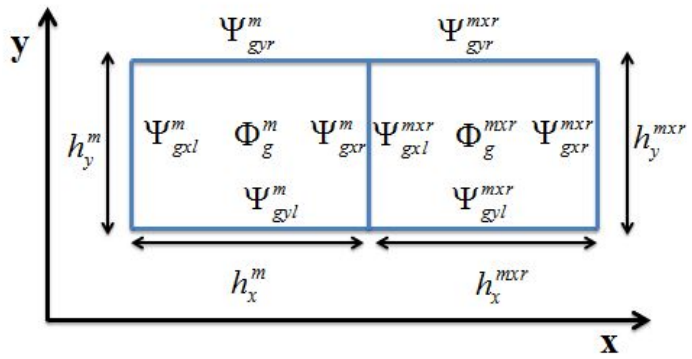

Figure 1: The nodal coordinate system for rectangular geometry.

2 Diffusion equation solution by NEM

2.1 Rectangular geometry

According to the literature (Bell and Glasstone, 1970), the steady-state neutron diffusion is presented in Eq. (1):

$$\begin{aligned}\vec{\nabla}.\vec{J_g} + \Sigma_{r,g}\phi_g(r) = &\sum_{\substack{g'=1\\ g'\neq g}}^{G} \Sigma_{s,g'g}\phi_{g'}(r) \\ &+ \frac{\chi_g}{k_{\text{eff}}}\sum_{g'=1}^{G}\nu\Sigma_{f,g'}\phi_{g'}(r)\end{aligned} \tag{1}$$

The discretization is performed using the average current nodal expansion method. First, to perform the calculations, the coordinate system in Fig. 1 should be defined and used.

On each considered axis and according to (Putney, 1986), the local dimensionless variable is defined as Eq. (2):

$$\begin{aligned}&\xi_u = \frac{u}{h_u}\\ &h_x = h_y = H\\ &u = x, y\end{aligned} \tag{2}$$

In the higher-order solution of the nodal expansion method for rectangular geometry, fourth-degree polynomials are used. In general, following Ref. (Kolali et al., 2021), the n^{th} order of polynomial expansion in the form of Eq. (3):

$$\begin{aligned}\Phi_g^{[n]} =&\Phi_g^{[0]} + \sum_{\substack{i=3\\ u=x,y}}^{n+2} d_{gui}\, h_i(\xi_u)\\ &+ \sum_{\substack{i,j=1\\ i+j\neq 2}}^{i+j\leq n+2} c_{g,ij}\, h_i(\xi_x)\, h_j(\xi_y)\ ;\ n\geq 1\end{aligned} \tag{3}$$

in which $h_i(\xi_u)$ are polynomials of i a degree from ξ_u, and each of these functions are selected to have orthogonal functions throughout the volume of the node Π^m. According to Fick Law, for Γ^m_{ul}:

$$\begin{aligned}j^{+m}_{gul} - j^{-m}_{gul} &= -\frac{1}{A^m_{ul}}\int \Gamma^m_{ul} D_g \nabla\phi_g e^m_{ul}\, \mathrm{d}\Gamma^m_{ul}\\ &= \frac{D^m_g}{h^m_u}(a_{gu} - b_{gu})\\ &= \frac{D^m_g}{h^m_u}(-2\Psi^m_{gur} - 4\Psi^m_{gul} + 6\Phi^m_g)\end{aligned} \tag{4}$$

In the diffusion approximation, surface flux is related to current according to the following equation:

$$\Psi^m_{gus} = 2\left(j^{+m}_{gus} - j^{-m}_{gus}\right) \tag{5}$$

By combining Eqs. (4) and (5), the following equation

is obtained:

$$\begin{bmatrix} j^{+m}_{gul} \\ j^{+m}_{gur} \end{bmatrix} = \begin{bmatrix} A^m_{gu} & B^m_{gu} & C^m_{gu} & -D^m_{gu} & E^m_{gu} \\ A^m_{gu} & C^m_{gu} & B^m_{gu} & D^m_{gu} & E^m_{gu} \end{bmatrix} \begin{bmatrix} \Phi^m_g \\ j^{-m}_{gul} \\ j^{-m}_{gur} \\ d^m_{gu1} \\ j^m_{gu2} \end{bmatrix} \tag{6}$$

Now using Eqs. (6), (1), and (3), the neutron balance equation is obtained as Eq. (7):

$$\begin{aligned} \Big[\sum_{u=x,y} 2\frac{A^m_{gu}}{h^m_u} + \Sigma^m_{r,g} \Big] \Phi^m_g = & \\ \sum_{\substack{g'=1 \\ g' \neq g}}^{G} \Sigma^m_{s,g'g} \Phi^m_{g'} + \frac{\chi_g}{k_{\text{eff}}} \sum_{g'=1}^{G} \nu\Sigma^m_{f,g'} \Phi^m_{g'} & \\ + \sum_{u=x,y} \frac{1}{h^m_u} \Big[\Big(1 - B^m_{gu} - C^m_{gu}\Big) \Big(j^{-m}_{gul} + j^{-m}_{gur}\Big) & \\ - 2E^m_{gu} d^m_{gu2} \Big] & \end{aligned} \tag{7}$$

In order to solve Eqs. (6) and (7), additional equations that include the first and the second-order coefficients, are needed. To obtain these coefficients, we can use weighted residual integrals. The remaining weighted integral for the m^{th} node is defined as Eq. (8):

$$\begin{aligned} \int_{-\frac{h^m_u}{2}}^{\frac{h^m_u}{2}} W_k(u) \Big[- D^m_g \frac{\mathrm{d}^2 \Psi^m_{gu}}{\mathrm{d}^2 u} + \Sigma_{r,g} \Psi^m_{gu} + L^m_{gu} & \\ - \sum_{\substack{g'=1 \\ g' \neq g}}^{G} \Sigma^m_{s,g'g} \Psi^m_{g'u} - \frac{\chi_g}{k_{\text{eff}}} \sum_{g'=1}^{G} \nu\Sigma^m_{f,g'} \Psi^m_{g'u} \Big] \mathrm{d}u = 0 & \end{aligned} \tag{8}$$

$W_k(u)$, the weighting function in the Eq. (8), can be chosen momentum (Eq. (9)) or Galerkin (Eq. (10)) weighting function.

$$\begin{aligned} W_1 &= h_1(\xi_u) = \xi_u \\ W_2 &= h_2(\xi_u) = \xi_u^2 - \frac{1}{12} \\ \xi_u &= \frac{u}{h} \;\; ; \;\; u = x, y \end{aligned} \tag{9}$$

$$\begin{aligned} W_1 &= h_3(\xi_u) = \xi_u \big(\xi_u^2 - \frac{1}{12}\big) \\ W_2 &= h_4(\xi_u) = \big(\xi_u^2 - \frac{1}{4}\big)\big(\xi_u^2 - \frac{1}{20}\big) \end{aligned} \tag{10}$$

After replacing in Eq. (8), for the higher-order coefficients, Eq. (11) is obtained:

$$\begin{aligned} \Big\{ \frac{D^m_g}{h^{m^2}_u} + A_k \Sigma^m_{r,g} \Big\} d^m_{guk} = \sum_{\substack{g'=1 \\ g' \neq g}}^{G} \Sigma^m_{s,g'g} \Big\{ A_k d^m_{g'uk} - B_k e^m_{g'uk} \Big\} & \\ + \frac{\chi_g}{k_{\text{eff}}} \sum_{g'=1}^{G} \nu\Sigma^m_{f,g'} \Big\{ A_k d^m_{g'uk} - B_k e^m_{g'uk} \Big\} & \\ + B_k \Sigma^m_{r,g} e^m_{guk} + B_k L^m_{guk} & \end{aligned} \tag{11}$$

2.2 *Hexagonal geometry*

To perform the calculations in hexagonal geometry, the coordinate system in Fig. 2 should be defined.

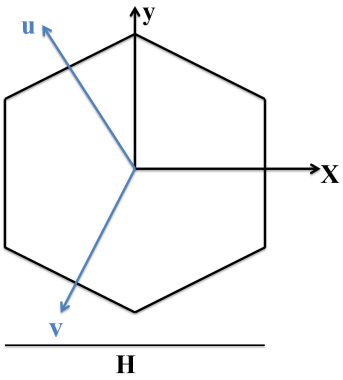

Figure 2: The nodal coordinate system for hexagonal geometry.

In the higher-order solution of the nodal expansion method for hexagonal geometry, fifth-degree polynomials are used. In general, in accordance with (Putney, 1986), the n^{th} order of polynomial expansion is defined as Eq. (12):

$$\begin{aligned} \phi^{[1]}_g &= \phi^{[0]}_g + d_{gx} h_5(\xi_x) + d_{gu} h_5(\xi_u) + d_{gv} h_5(\xi_v) \\ &= A_g h_0 + a_{gx} h_1(\xi_x) + b_{gx} h_2(\xi_x) + a_{gu} h_1(\xi_u) \\ &+ b_{gu} h_2(\xi_u) + a_{gv} h_1(\xi_v) + b_{gv} h_2(\xi_v) \\ &+ c_g h_1(\xi_x) h_1(\xi_u) h_1(\xi_v) + d_{gx} h_5(\xi_x) \\ &+ d_{gu} h_5(\xi_u) + d_{gv} h_5(\xi_v) \end{aligned} \tag{12}$$

According to Fick Law, for Γ^m_{xr}:

$$\begin{aligned} j^{+m}_{gxr} - j^{-m}_{gxr} = -\frac{D^m_g}{H} \Big[\frac{47}{5} (j^{+m}_{gxr} + j^{-m}_{gxr}) & \\ + \frac{7}{5} (j^{+m}_{gxl} + j^{-m}_{gxl}) + \frac{29}{10} (j^{+m}_{gur} + j^{-m}_{gur}) & \\ - \frac{11}{10} (j^{+m}_{gul} + j^{-m}_{gul}) + \frac{29}{10} (j^{+m}_{gvr} + j^{-m}_{gvr}) & \\ - \frac{11}{10} (j^{+m}_{gvl} + j^{-m}_{gvl}) - \frac{36}{5} \Phi^m_g + \frac{1}{12} d_{gx} \Big] & \end{aligned} \tag{13}$$

By combining Eqs. (4) and (13), the coupling equation is obtained as Eq. (14):

$$\begin{bmatrix} j^{+m}_{gxr} \\ j^{+m}_{gxl} \\ j^{+m}_{gur} \\ j^{+m}_{gul} \\ j^{+m}_{gvr} \\ j^{+m}_{gvl} \end{bmatrix} = \begin{bmatrix} C^m_{g1} & C^m_{g2} & C^m_{g4} & C^m_{g3} & C^m_{g4} & C^m_{g3} & C^m_{g5} \\ C^m_{g2} & C^m_{g1} & C^m_{g3} & C^m_{g4} & C^m_{g3} & C^m_{g4} & C^m_{g5} \\ C^m_{g4} & C^m_{g3} & C^m_{g1} & C^m_{g2} & C^m_{g4} & C^m_{g3} & C^m_{g5} \\ C^m_{g3} & C^m_{g4} & C^m_{g2} & C^m_{g1} & C^m_{g3} & C^m_{g4} & C^m_{g5} \\ C^m_{g4} & C^m_{g3} & C^m_{g4} & C^m_{g3} & C^m_{g1} & C^m_{g2} & C^m_{g5} \\ C^m_{g3} & C^m_{g4} & C^m_{g3} & C^m_{g4} & C^m_{g2} & C^m_{g1} & C^m_{g5} \end{bmatrix} \begin{bmatrix} j^{-m}_{gxr} \\ j^{-m}_{gxl} \\ j^{-m}_{gur} \\ j^{-m}_{gul} \\ j^{-m}_{gvr} \\ j^{-m}_{gvl} \\ \Phi^m_g \end{bmatrix} \tag{14}$$

Now using Eqs. (14), (1), and (12), the neutron balance equation is obtained as Eq. (15):

$$\begin{aligned}&\Big[\frac{4}{H}C^m_{g5}+\Sigma^m_{rg}\Big]\Phi^m_g\\&=\sum_{\substack{g'=1\\g'\neq g}}^{G}\Sigma^m_{sg'g}\Phi^m_{g'}+\frac{\chi_g}{k_{\text{eff}}}\sum_{g'=1}^{G}\nu\Sigma^m_{fg'}\Phi^m_{g'}\\&+\sum_{\substack{s=r,l\\w=x,u,v}}\frac{2}{3h}\Big(1-C^m_{g1}-C^m_{g2}-2C^m_{g3}-2C^m_{g4}\Big)j^{-m}_{gws}\end{aligned}\tag{15}$$

In order to solve Eqs. (14) and (15), additional equations that include the high order coefficients are needed. To obtain these coefficients one can use weighted residual integrals. The remaining weighted integral for the m node is defined as Eq. (16):

$$\begin{aligned}\int_{\Pi^m}W(\xi_w)\Big[&-D_g\nabla^2\phi_g+\Sigma_{r,g}\phi_g-\sum_{\substack{g'=1\\g'\neq g}}^{G}\Sigma^m_{gg'}\phi_{g'}\\&-\frac{\chi_g}{k_{\text{eff}}}\sum_{g'=1}^{G}\nu\Sigma^m_{f,g'}\phi_{g'}\Big]\,\mathrm{d}\Pi^m=0\end{aligned}\tag{16}$$

$W(u)$ weighting function can be chosen as momentum (Eq. (17)) or Galerkin (Eq. (18)) weighting functions:

$$\begin{aligned}w&=h_3(\xi_w)=\xi_w\big(\xi_w^2-\frac{1}{4}\big)\\\xi_w&=\frac{w}{h}\quad;\quad w=x,u,v\end{aligned}\tag{17}$$

$$\begin{aligned}w&=h_5(\xi_w)=\xi_w\big(\xi_w^2-\frac{1}{4}\big)\big(\xi_w^2-\frac{1}{12}\big)\\&=\xi_w^5-\frac{1}{3}\xi_w^3+\frac{1}{48}\xi_w\end{aligned}\tag{18}$$

After replacing in Eq. (16), for the higher order coefficients, Eqs. (19) and (20) are obtained:

$$\begin{bmatrix}\alpha^m_g&\beta^m_g&\beta^m_g\\\beta^m_g&\alpha^m_g&\beta^m_g\\\beta^m_g&\beta^m_g&\alpha^m_g\end{bmatrix}\begin{bmatrix}d_{gx}\\d_{gu}\\d_{gv}\end{bmatrix}=\begin{bmatrix}Q^m_{gx}\\Q^m_{gu}\\Q^m_{gv}\end{bmatrix}\tag{19}$$

$$\begin{aligned}Q^m_{gx}&=\Sigma^m_{rg}\Big\{\frac{233}{36}\tilde{a}_{gx}+\frac{1}{8}\tilde{c}_g\Big\}\\&+\sum_{\substack{g'=1\\g'\neq g}}^{G}\Sigma^m_{gg'}\Big(-\frac{233}{36}\tilde{a}_{g'x}-\frac{1}{8}\tilde{c}_{g'}+\frac{179}{4752}\tilde{d}_{g'x}\\&+\frac{49}{19008}\tilde{d}_{g'u}+\frac{49}{19008}\tilde{d}_{g'v}\Big)\\&+\frac{\chi_g}{k_{\text{eff}}}\sum_{g'=1}^{G}\nu\Sigma^m_{fg'}\Big(-\frac{233}{36}\tilde{a}_{g'x}-\frac{1}{8}\tilde{c}_{g'}\\&+\frac{179}{4752}\tilde{d}_{g'x}+\frac{49}{19008}\tilde{d}_{g'u}+\frac{49}{19008}\tilde{d}_{g'v}\Big)\end{aligned}\tag{20}$$

2.3 Adjoint equation solution by NEM

For considering the point detector and source, the neutron flux distribution is equal to the adjoint one. Before solving the adjoint diffusion equation, it should be noted that the adjoint operator is the transpose of the forward operator. Therefore, the neutron diffusion equation in operator format is defined as Eq. (21) and the matrix form of the adjoint diffusion equation is obtained as Eq. (22):

$$L\phi=\frac{1}{k_{\text{eff}}}F\phi\tag{21}$$

$$L^\dagger\phi^\dagger=\frac{1}{k^\dagger_{\text{eff}}}F^\dagger\phi^\dagger\tag{22}$$

in which L and F are called loss operator and fission operator that $L^\dagger$ and $F^\dagger$ are the transpose of them. Also, $\phi^\dagger$ refers to the adjoint flux and $k^\dagger_{\text{eff}}$ adjoint effective multiplication factor. It should be noted that in the steady-state calculations $k^\dagger_{\text{eff}}$ is equal to k_{eff}. To solve the adjoint equations, the method for the discretization of equations is similar to the forward scheme.

2.4 Programming algorithm

By obtaining a complete set of forward and adjoint nodal equations, the neutron flux distribution in each energy group and the relative power distribution, as well as the effective neutron multiplication factor, are obtained from solving the system of equations.

Since the nodal balance equation is obtained by placing the nodal correlated equations within the neutron diffusion equation, the governing equations are interdependent. In other words, both the system of equations obtained are of the eigenvalue type, and the correlated equations and the nodal balance are not independent (Kolali et al., 2021); Therefore, the power iteration algorithm should be used in programming. The power iteration algorithm for solving the diffusion equation based on the nodal method of high-order flux expansion for rectangular and hexagonal geometry is shown by (Kolali et al., 2020) and (Kolali et al., 2019), respectively. Also, the convergence criteria are considered equal to 10^{-7} to calculate the effective multiplication factor and 10^{-5} for the neutron flux distribution.

3 Benchmarking and Results

In order to ensure the discretization method as well as to check the accuracy of the developed programs, calculations for the benchmark reactors core BIBLIS-2D (Smith, 1979) for rectangular geometry and IAEA-2D (Hebert, 2008; Chao and Shatilla, 1995; Grundmann and Hollstein, 1999) for hexagonal geometry with given macroscopic cross-sections were done.

Figure 3 shows the arrangement of fuel assemblies in the core of the reactors. The number in each of the assemblies indicates the material numbers, and the materials specifications can be seen in Tables 1 and 2, respectively.

Table 1: Two-group (thermal and fast) constants for the core of the BIBLIS-2D reactor (Hosseini et al., 2018).

Group-wise Constants	M #1	M #2	M #3 (R)	M #4	M #5	M #6	M #7	M #8
D_1 (cm)	1.4360	1.4366	1.3200	1.4389	1.4381	1.4385	1.4389	1.4349
D_2 (cm)	0.3635	0.3636	0.02772	0.03638	0.3665	0.3665	0.3679	0.3680
$\nu\Sigma_{f,1}$ (cm^{-1})	0.0058	0.0061	0.0	0.0074	0.0061	0.0064	0.0061	0.0064
$\nu\Sigma_{f,2}$ (cm^{-1})	0.0960	0.1035	0.0	0.1323	0.1035	0.1091	0.1035	0.1091
$\Sigma_{a,1}$ (cm^{-1})	0.0095	0.0096	0.0026	0.0103	0.0100	0.0101	0.0101	0.0102
$\Sigma_{a,2}$ (cm^{-1})	0.0750	0.0784	0.0715	0.0914	0.0848	0.0873	0.0880	0.0905
$\Sigma_{s,12}$ (cm^{-1})	0.0171	0.0172	0.0173	0.0171	0.0231	0.0176	0.0177	0.0170

Table 2: Two-group (thermal and fast) constants for the core of the IAEA-2D reactor (Kolali et al., 2019).

Group-wise Constants	M #1	M #2	M #3	M #4
D_1 (cm)	1.5	1.5	1.5	1.5
D_2 (cm)	0.4	0.4	0.4	0.4
$\nu\Sigma_{f,1}$ (cm^{-1})	0.0	0.0	0.0	0.0
$\nu\Sigma_{f,2}$ (cm^{-1})	0.135	0.135	0.135	0.0
$\Sigma_{a,1}$ (cm^{-1})	0.01	0.01	0.01	0.0
$\Sigma_{a,2}$ (cm^{-1})	0.08	0.085	0.13	0.01
$\Sigma_{s,12}$ (cm^{-1})	0.02	0.02	0.02	0.04

Table 3: Calculated effective multiplication factors and relative power values.

		k_{eff}	k_{eff} Error (pcm)	Max. ERP (%)	Ave. ERP (%)
BIBLIS-2D	Momentum weighting functions	1.02534	21	1.18	0.42
	Galerkin weighting functions	1.02540	27	1.45	0.62
IAEA-2D	Momentum weighting functions	1.00420	129	11.88	4.96
	Galerkin weighting functions	1.00534	16	8.88	3.52

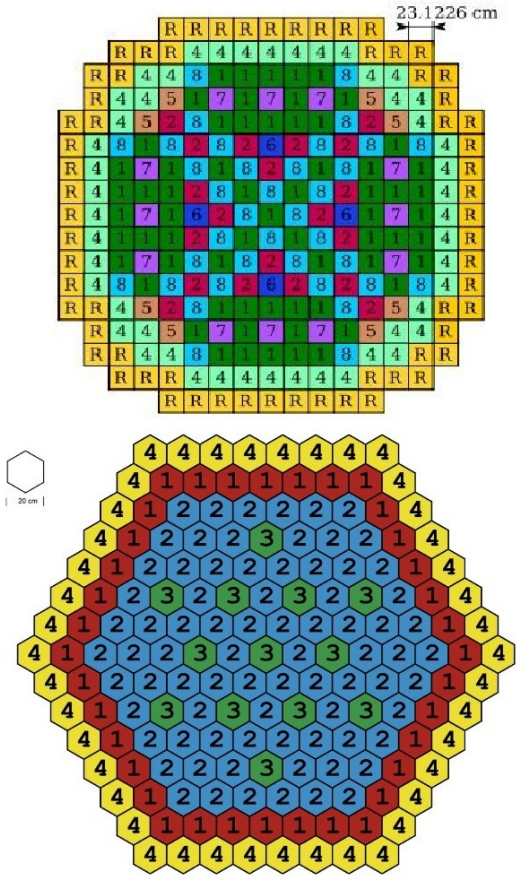

Figure 3: Arrangement of fuel assemblies in the cores of BIBLIS-2D reactor (above) and IAEA-2D reactor (bottom) (Putney, 1986).

According to the references, the boundary condition for the core of the BIBLIS-2D reactor is considered as vacuum boundary condition. Calculations for the core of this reactor were performed with nodes the size of a fuel assembly and for two weighting functions of momentum and Galerkin, which results are reported in Table 3. Also, in Table 3, the maximum and average error of the relative power distribution (ERP) are reported for the momentum and Galerkin weighting functions. Figure 4 shows the neutron flux distribution in the thermal and fast groups, and Fig. 5 shows the distribution of the adjoint flux in the thermal and fast group in the BIBLIS-2D reactor for the momentum weighting function.

For the IAEA-2D benchmark reactor, calculations were performed with nodes the size of a fuel assembly and an albedo boundary condition of 0.5, and for the momentum and Galerkin weighting functions, and results are reported in Table 3. Figure 6 shows the neutron flux distribution, and Fig. 7 shows the adjoint flux distribution in this reactor for the Galerkin weighting function.

As can be seen from Table 3, for reactors with hexagonal geometry, the Galerkin weighting function has better accuracy than the momentum weighting function, and the momentum weighting function are more suitable for reactors with rectangular geometriy.

4 Conclusions

To analyze and perform neutronic calculations of nuclear reactors, it is necessary to develop software to calculate

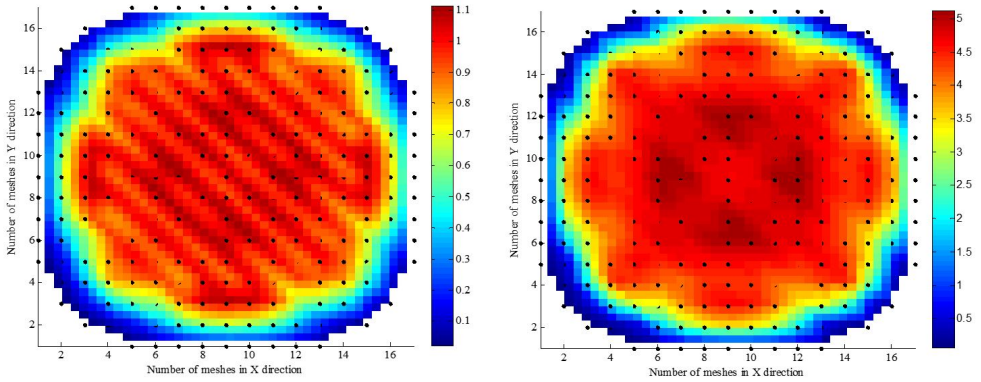

Figure 4: Distribution of the neutron flux in thermal (left) and fast (right) groups.

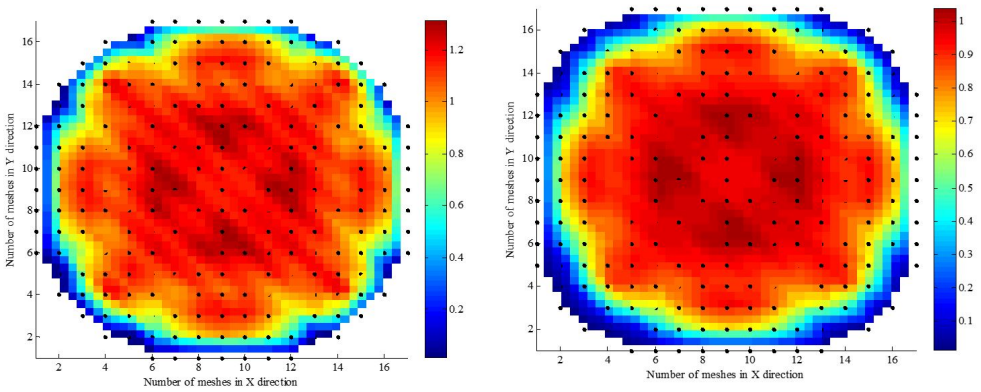

Figure 5: Distribution of the adjoint neutron flux in thermal (left) and fast (right) groups.

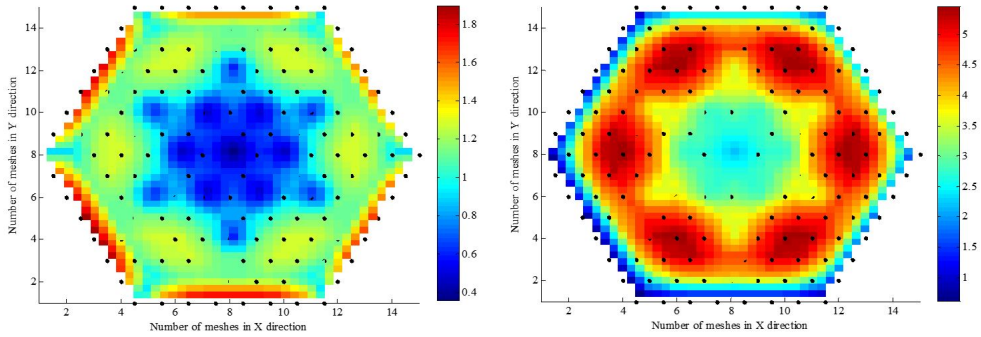

Figure 6: Distribution of the neutron flux in thermal (left) and fast (right) groups.

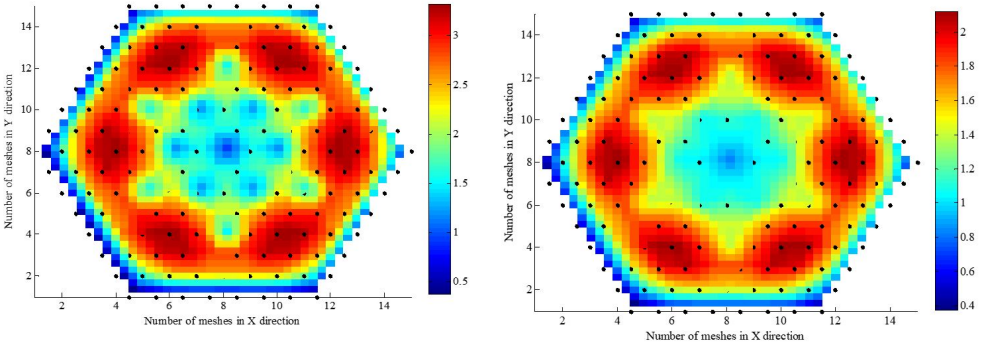

Figure 7: Distribution of the adjoint neutron flux in thermal (right) and fast (left) groups.

the distribution of core power, which has efficient and fast methods. Since, in the case of time-dependent calculations, due to time discretization, in addition to spatial discretization, the cost and time of calculations are significantly increased, the use of the high-order flux expansion nodal method with nodes in the dimensions of a fuel assembly is beneficial because they have both the proper speed and accuracy. In order to verify and compare the two momentum and Galerkin weighting functions, calculations were performed for the core of BIBLIS-2D reactor as a benchmark problem for the reactors with rectangular geometry, and for the core of IAEA-2D reactor as a benchmark problem for reactors with hexagonal geometry. The results show that for the reactors with rectangular geometry, the momentum and Galerkin weighting functions have almost the same accuracy because, for the BIBLIS-2D reactor, the mean relative power distribution error for the momentum and Galerkin weighting functions was 0.42% and 0.62%, respectively. Also, according to Table 3, their effective multiplication factors were obtained close to each other.

For the reactors with hexagonal geometry, the Galerkin weighting function results in much more accurate answers, because for the IAEA-2D reactor, the average relative power distribution error for the momentum and Galerkin weighting functions was 4.96% and 3.52%, respectively, and according to Table 3, the error of the effective neutron multiplication factor for the Galerkin weighting function was about 100 pcm less.

Regarding the results, it was concluded that in order to increase accuracy with the acceptable time of computing (4 seconds for rectangular geometry and 28 seconds for hexagonal geometry with Intel® Core™ i7-4510U Processor), the Momentum weighting function for rectangular geometry and the Galerkin weighting function for hexagonal geometry can be used to discretize equations without reducing the node size.

Therefore, in order to increase the accuracy while maintaining the speed of calculations, without reducing the size of nodes, the appropriate weighting function could be used in discretization, which can be very useful in performing calculations of different transients.

References

Bell, G. I. and Glasstone, S. (1970). Nuclear reactor theory. Technical report, US Atomic Energy Commission, Washington, DC (United States).

Chao, Y. A. and Shatilla, Y. (1995). Conformal mapping and hexagonal nodal methodsII: implementation in the ANC-H code. *Nuclear Science and Engineering*, 121(2):210–225.

Finnemann, H. (1975). A consistent Nodal Method for the Analysis of Space-Time Effects in large LWR's. Technical report.

Grundmann, U. and Hollstein, F. (1999). A two-dimensional intranodal flux expansion method for hexagonal geometry. *Nuclear Science and Engineering*, 133(2):201–212.

Hall, S. (2013). The Development of a Nodal Method for the Analysis of PWR Cores with Advanced Fuels.

Hebert, A. (2008). A Raviart–Thomas–Schneider solution of the diffusion equation in hexagonal geometry. *Annals of Nuclear Energy*, 35(3):363–376.

Hosseini, S. A. and Vosoughi, N. (2012). Neutron noise simulation by GFEM and unstructured triangle elements. *Nuclear Engineering and Design*, 253:238–258.

Hosseini, S. A., Vosoughi, N., and Vosoughi, J. (2018). Neutron noise simulation using ACNEM in the hexagonal geometry. *Annals of Nuclear Energy*, 113:246–255.

Kolali, A., Naghavi, D., and Vosoughi, N. (2019). Development of the SH3-ACNEM Simulator Program in order to Solving the Forward and Adjoint Neutron Diffusion Equation for Hexagonal Geometry Reactor Cores, Journal of Nuclear Science and Technology, In Press.

Kolali, A., Naghavi, D., and Vosoughi, N. (2020). Development of the S3-HACNEM Simulator Program in order to Solving the Forward and Adjoint Neutron Diffusion Equation for Rectangular Geometry Reactor Cores, Journal of Nuclear Science and Technology, In Press.

Kolali, A., Vosoughi, J., and Vosoughi, N. (2021). Development of SD-HACNEM neutron noise simulator based on high order nodal expansion method for rectangular geometry. *Annals of Nuclear Energy*, 162:108496.

Lawrence, R. D. (1983). DIF3D nodal neutronics option for two-and three-dimensional diffusion theory calculations in hexagonal geometry.[LMFBR]. Technical report, Argonne National Lab., IL (USA).

Putney, J. (1986). A hexagonal geometry nodal expansion method for fast reactor calculations. *Progress in Nuclear Energy*, 18(1-2):113–121.

Sims, R. N. (1977). *A coarse-mesh nodal diffusion method based on response matrix considerations.* PhD thesis, Massachusetts Institute of Technology.

Smith, K. S. (1979). *An analytic nodal method for solving the two-group, multidimensional, static and transient neutron diffusion equations.* PhD thesis, Massachusetts Institute of Technology.